- Hierarchical Helical Assembly of Conjugated Poly(3-hexylthiophene)-block-poly(3-triethylene glycol thiophene) Diblock Copolymers
  Lee, E.; Hammer, B.; Kim, J.-K.; Page, Z.; Emrick, T.; Hayward, R. C. *J. Am. Chem. Soc.* **2011**, *133*, 10390-10393.
  Abstract:

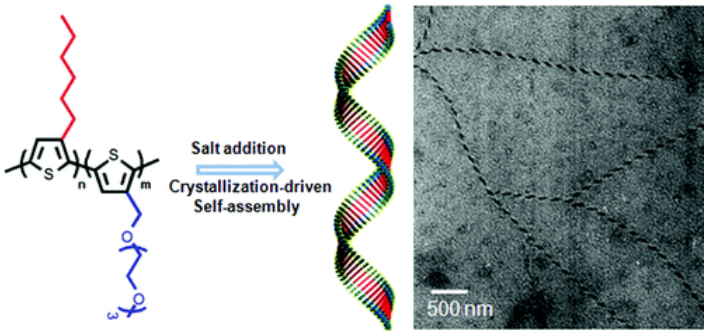

We report on the solution-state assembly of all-conjugated polythiophene diblock copolymers containing nonpolar (hexyl) and polar (triethylene glycol) side chains. The polar substituents provide a large contrast in solubility, enabling formation of stably suspended crystalline fibrils even under very poor solvent conditions for the poly(3-hexylthiophene) block. For appropriate block ratios, complexation of the triethylene glycol side chains with added potassium ions drives the formation of helical nanowires that further bundle into superhelical structures.

- Graphene Nanoribbons from Unzipped Carbon Nanotubes: Atomic Structures, Raman Spectroscopy, and Electrical Properties
  Xie, L.; Wang, H.; Jin, C.; Wang, X.; Jiao, L.; Suenaga, K.; Dai, H. *J. Am. Chem. Soc.* **2011**, *133*, 10394-10397.
  Abstract:

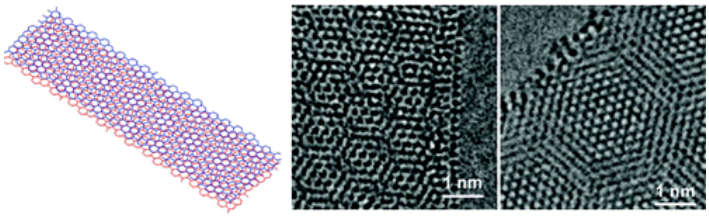

We investigated the atomic structures, Raman spectroscopic and electrical transport properties of individual graphene nanoribbons (GNRs, widths 10–30 nm) derived from sonochemical unzipping of multiwalled carbon nanotubes (MWNTs). Aberration-corrected transmission electron microscopy (TEM) revealed a high percentage of two-layer (2 L) GNRs and some single-layer ribbons. The layer–layer stacking angles ranged from 0° to 30° including average chiral angles near 30° (armchair orientation) or 0° (zigzag orientation). A large fraction of GNRs with bent and smooth edges was observed, while the rest showed flat and less smooth edges (roughness ≤1 nm). Polarized Raman spectroscopy probed individual GNRs to reveal D/G ratios and ratios of D band intensities at parallel and perpendicular laser excitation polarization ($D_{||}/D_{\perp}$). The observed spectroscopic trends were used to infer the average chiral angles and edge smoothness of GNRs. Electrical transport and Raman measurements were carried out for individual ribbons to correlate spectroscopic and electrical properties of GNRs.

- Self-Assembled Hollow Nanospheres Strongly Enhance Photoluminescence

Ke, D.; Zhan, C.; Xu, S.; Ding, X.; Peng, A.; Sun, J.; He, S.; Li, A. D. Q.; Yao, J. *J. Am. Chem. Soc.* **2011**, *133*, 11022–11025.

Abstract:

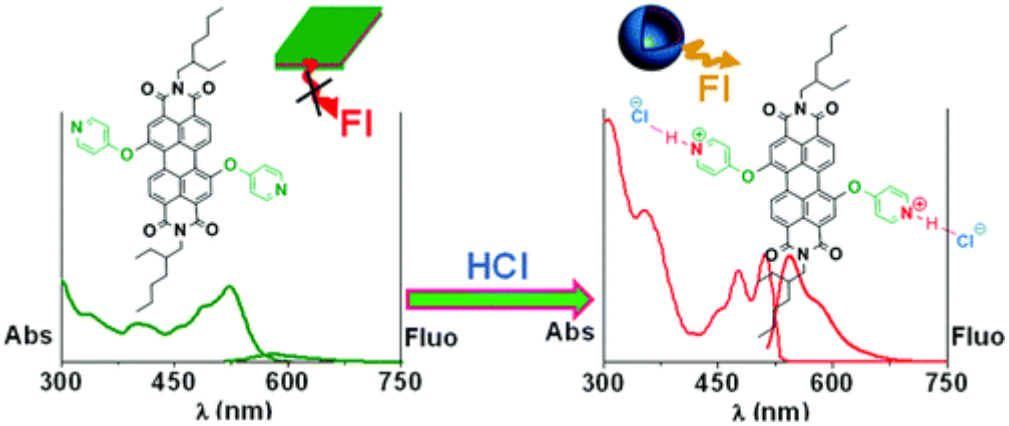

We report that two molecular building blocks differ only by two protons, yet they form totally different nanostructures. The protonated one self-organized into hollow nanospheres (~200 nm), whereas the one without the protons self-assembled into rectangular plates. Consequently, the geometrically defined nanoassemblies exhibit radically different properties. As self-assembly directing units, protons impart ion-pairing and hydrogen-bonding probabilities. The plate-forming nanosystem fluoresces weakly, probably due to energy transfer among chromophores ($\Phi < 0.2$), but the nanospheres emit strong yellow fluorescence ($\Phi \approx 0.58–0.85$).

- Thermoresponsive Dynamers: Thermally Induced, Reversible Chain Elongation of Amphiphilic Poly(acylhydrazones)
  Folmer-Andersen, J. F.; Lehn, J.-M. *J. Am. Chem. Soc.* **2011**, *133*, 10966–10973.
  Abstract:

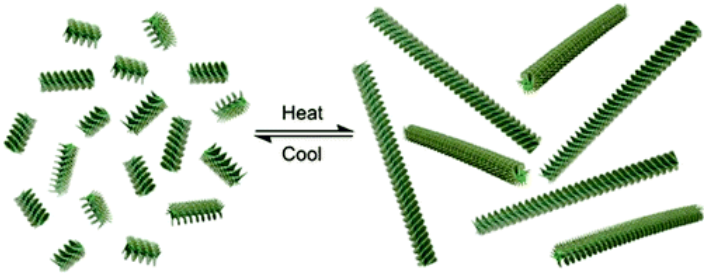

A nanostructured poly(acylhydrazone), which is reversibly formed in acidic aqueous solution from di(aldehyde) and di(acylhydrazine) monomers with appended hexaglyme groups, was found to display lower critical solution (LCS) behavior. Remarkably, under acidic conditions in which polymerization is reversible, large and reversible molecular weight (M_w) increases were observed in response to elevated temperatures, both below and above the LCS temperature. No variation in M_w was evident under neutral and alkaline conditions, in which the acylhydrazone condensation is essentially irreversible. Results of turbidometry studies, size-exclusion chromatography–multiangle laser light scattering (SEC–MALLS), and transmission electron microscopy (TEM) suggest that heating the polymer below the LCS temperature leads to polymer growth with preservation of the characteristic nanostructured morphology, whereas the onset of the microphase separated state causes a fundamental change in morphology, in which the polymer chains aggregate into larger bundles and fibers. van't Hoff analysis of a small molecule model system indicates that the acylhydrazone condensation is enthalpy driven ($\Delta H_{eq} = -8.2 \pm 0.2$ kcal·mol^{-1} and $\Delta S_{eq} = -11.1 \pm 0.4 =$

cal·mol^{-1}·K^{-1}), which suggests that the observed polymer growth with temperature is not a consequence of the intrinsic thermodynamics of the intermonomer linkage but is likely the result of the thermoresponsive characteristics conferred by the multiple hexaglyme groups. The system described displays double control of the dynamer state by two orthogonal agents, heat and protons (pH). It also represents a prototype for dynamic materials displaying multiple control adaptive behavior.

- Design and Synthesis of Sphingomyelin–Cholesterol Conjugates and Their Formation of Ordered Membranes
  Matsumori, N.; Tanada, N.; Nozu, K.; Okazaki, H.; Oishi, T.; Murata, M. *Chem. Eur. J.* **2011**, *17,* 8568-8575.
  Abstract:

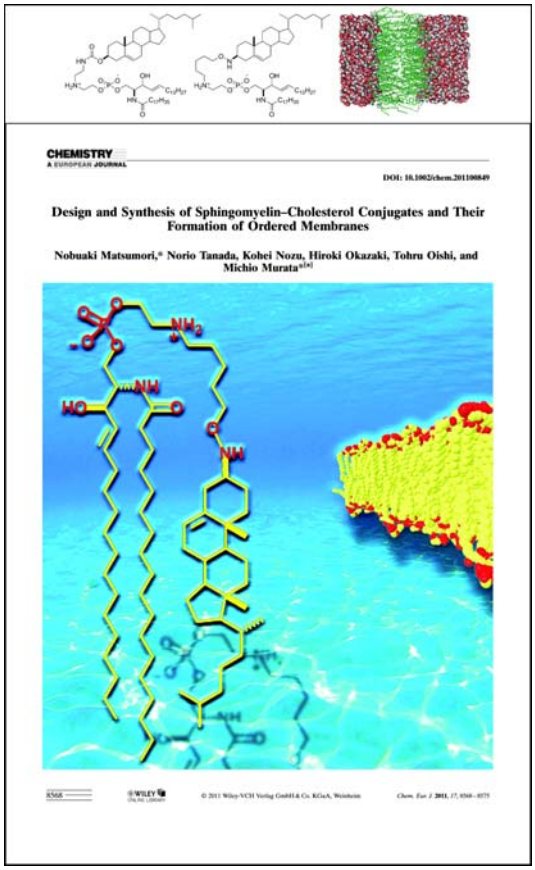

A lipid raft is a cholesterol (Chol)-rich microdomain floating in a sea of lipid bilayers. Although Chol is thought to interact preferentially with sphingolipids such as sphingomyelin (SM), rather than with glycerophospholipids, the origin of the specific interaction has remained unresolved, primarily because of the high mobility of lipid molecules and weak intermolecular interactions. In this study, we synthesized SM–Chol conjugates with functionally designed linker portions to restrain Chol mobility and examined their formation of ordered membranes by a detergent insolubility assay, fluorescence anisotropy experiments, and fluorescence-quenching assay. In all of the tests, membranes prepared from the conjugates showed properties of ordered domains comparable to a SM–Chol (1:1) membrane. To gain insight into the structure of bilayers composed from the conjugates, we performed molecular dynamics simulations with 64 molecules of the conjugates, which suggested that the conjugates form a stable bilayer structure by bending at the linker portion and, mostly, reproduce the hydrogen bonds between the SM and Chol portions. These results imply

that the molecular recognition between SM and Chol in an ordered domain is essentially reproduced by the conjugated molecules and, thus, demonstrates that these conjugate molecules could potentially serve as molecular probes for understanding molecular recognition in lipid rafts.

- Rational Design of Zinc–Organic Coordination Polymers Directed by N-Donor Co-ligands
  Wang, S.; Xiong, S.; Wang, Z.; Du, J. *Chem. Eur. J.* **2011**, *17,* 8630-8642.
  Abstract:

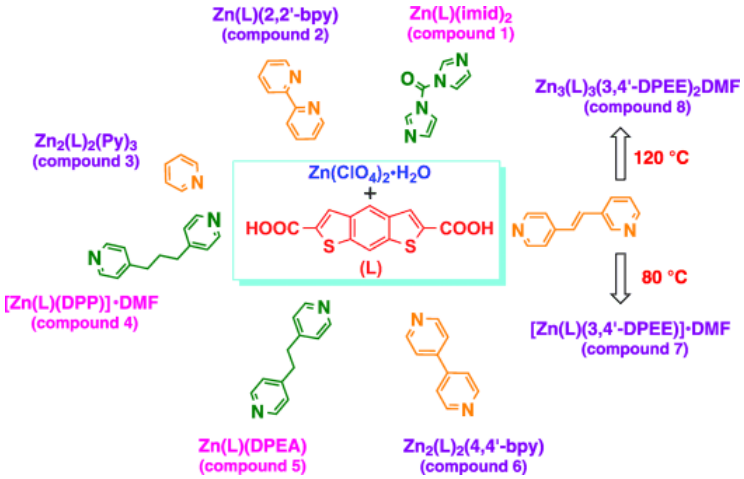

A family of ZnII-based metal–organic coordination polymers (MOCPs) [Zn(L)(imid)$_2$] (1), [Zn(L)(2,2′-bpy)] (2), [Zn$_2$(L)$_2$(Py)$_3$] (3), [Zn(L)(DPP)]□DMF (4), [Zn(L)(DPEA)] (5), [Zn$_2$(L)$_2$(4,4′-bpy)] (6), [Zn(L)(3,4′-DPEE)]□DMF (7), and [Zn$_3$(L)$_3$(3,4′-DPEE)2]□DMF (8) (L=dithieno[3,2-*b*:2′,3′-*e*]benzene-2,6-dicarboxylic acid, imid=imidazole, bpy=bipyridine, Py=pyridine, DPP=1,3-di(pyridin-4-yl)propane, DPEA=1,2-di(pyridin-4-yl)ethane, and DPEE=(*E*)-3,4′-(ethene-1,2-diyl)dipyridine) have been rationally designed and generated in the solvothermal reaction systems of the new conjugated thiophene derivative L, Zn(ClO$_4$)$_2$□6□H$_2$O, and seven different aromatic N-donor co-ligands separately. These N-donor compounds were carefully selected and employed in the crystal preparation of the eight MOCPs as structure-directing co-ligands owing to their structural specialties and habitual coordination fashions. Among these MOCPs, compounds 1–3 are 1D polymers with different chain structures. Compounds 4, 7, and 8 are 2D structures, in which 4 has two sets of twofold interpenetrating layers, whereas 7 and 8 are both built from three independent sheets. Compounds 5 and 6 are 3D frameworks, in which 5 exhibits a fivefold interpenetrating diamondoid network, whereas 6 shows a typical twofold interpenetrating pillared layer structure with nanoscale channels. The photoluminescent properties of these MOCPs, including excitation, emission, and radiactive lifetime, have also been investigated to help us tentatively understand their structure–property relationships.

- Supramolecular construction of vesicles based on core-substituted naphthalene diimide appended with triethyleneglycol motifs
  Bhosale, S. V.; Jani, C. H.; Lalander, C. H.; Langford, S. J.; Nerush, I.; Shapter, J. G.; Villamaina, D.; Vauthey, E. *Chem. Commun.* **2011**, *47*, 8226-8228.
  Abstract:

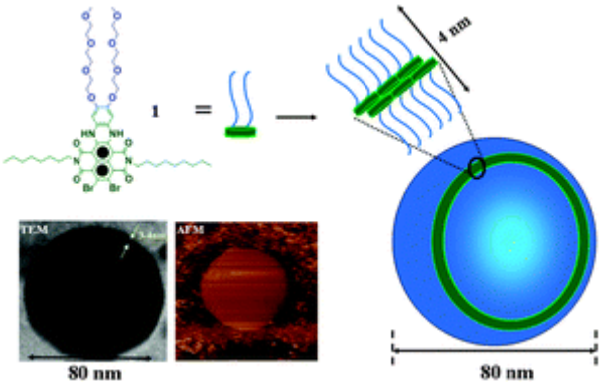

The supramolecular self-assembly of core-substituted NDIs bearing triethylene glycol motifs leads to the formation of stable vesicles in DMSO and $CHCl_3$/MeOH (6 : 4, *v*/*v*) solvent mixes.

- An amphiphilic pyrene sheet for selective functionalization of graphene
  Lee, D.-W.; Kim, T.; Lee, M. *Chem. Commun.* **2011**, *47*, 8259-8261.
  Abstract:

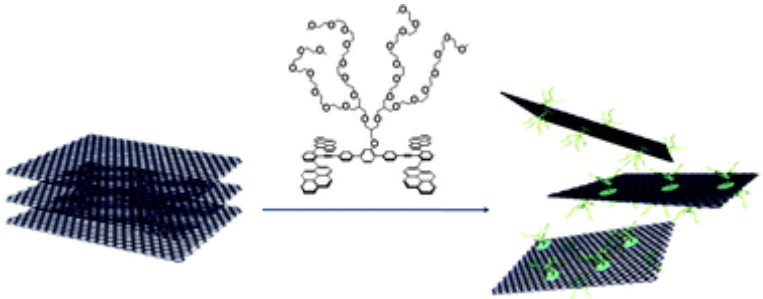

The amphiphile aromatic sheet can selectively exfoliate graphite powder into single and double layer graphene sheets.

- Structural changes in block copolymer micelles induced by cosolvent mixtures
  Kelley, E.; Smart, T.; Jackson, A.; Sullivan, M.; Epps, T. *Soft Matter* **2011**, *7*, 7094-7102.
  Abstract:

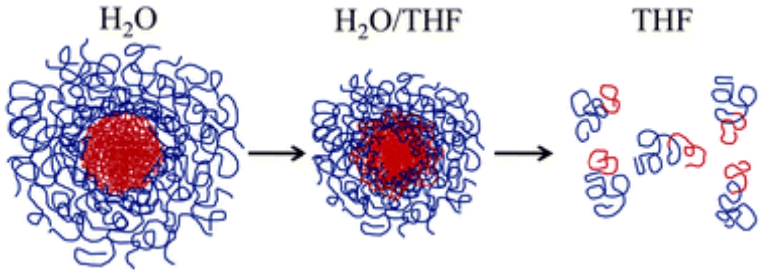

We investigated the influence of tetrahydrofuran (THF) addition on the structure of poly(1,2-butadiene-b-ethylene oxide) [PB-PEO] micelles in aqueous solution. Our studies showed that while the micelles remained starlike, the micelle core-corona interfacial tension and micelle size decreased upon THF addition. The detailed effects of the reduction in interfacial tension were probed using contrast variations in small angle neutron scattering (SANS) experiments. At low THF contents (high interfacial tensions), the SANS data were fit to a micelle form factor that incorporated a radial density distribution of corona chains to account for the starlike micelle profile. However, at higher THF contents (low interfacial tensions), the presence of free chains in solution affected the scattering at high q and required the implementation of a linear combination of micelle and Gaussian coil form factors. These SANS data fits indicated that the reduction in interfacial tension led to broadening of

the core-corona interface, which increased the PB chain solvent accessibility at intermediate THF solvent fractions. We also noted that the micelle cores swelled with increasing THF addition, suggesting that previous assumptions of the micelle core solvent content in cosolvent mixtures may not be accurate. Control over the size, corona thickness, and extent of solvent accessible PB in these micelles can be a powerful tool in the development of targeting delivery vehicles.

- Photo-induced micellization of block copolymers bearing 4,5-dimethoxy-2-nitrobenzyl side groups
  Bertrand, O.; Schumers, J.; Kuppan, C.; Marchand-Brynaert, J.; Fustin, C.; Gohy, J. *Soft Matter* **2011**, *7*, 6891-6896.
  Abstract:

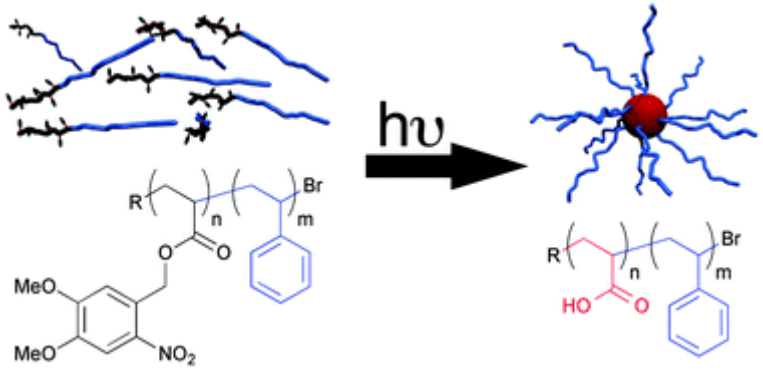

The synthesis of photocleavable poly(dimethoxynitrobenzyl acrylate)-block-polystyrene block copolymers is described. The UV irradiation of these block copolymers, dissolved in a good solvent for both blocks, selectively cleaves the dimethoxynitrobenzyl protecting groups, leading to carboxylic acid moieties. Since the resulting hydrophilic poly(acrylic acid) block is insoluble in the solvent used, self-assembly of the diblocks into micelles is observed. This light-induced micellization process is further used to trap dyes into the core of the micelles.

- Graphene: Materials in the Flatland (Nobel Lecture)
  Novoselov, K. S. *Angew. Chem. Int. Ed.* **2011**, *50*, 6986–7002.
  Abstract:

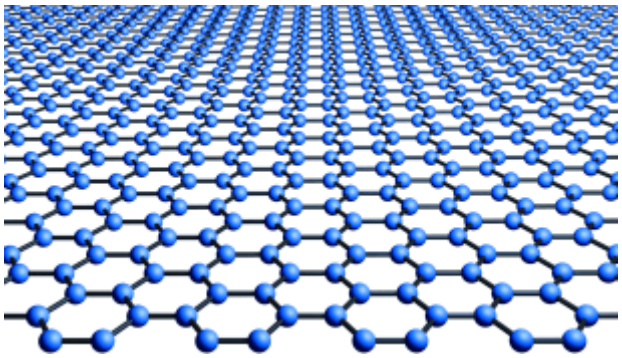

Much like the world described in Abbott's "Flatland", graphene is a two-dimensional object. And, as "Flatland" is "A Romance of Many Dimensions", graphene is much more than just a flat crystal. It possesses a number of unusual properties which are often unique or superior to those in other materials. In this brief lecture I would like to explain the reason for my (and many other people's) fascination with this material, and invite the reader to share some of the excitement I've experienced while researching it.

- Magical Power of Transition Metals: Past, Present, and Future (Nobel Lecture)
  Negishi, E.-i. *Angew. Chem. Int. Ed.* **2011**, *50*, 6738–6764.
  Abstract:

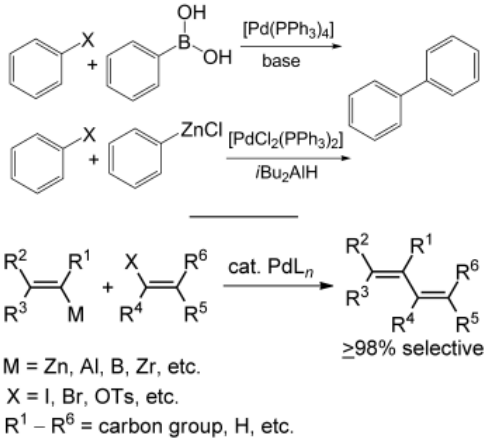

The Nobel Prize in Chemistry 2010 was awarded for research on palladium-catalyzed cross-coupling in organic synthesis. Two of the Laureates, A. Suzuki and E. Negishi, report here first hand on the historical development and the current status of this research.

- *n*-Channel Semiconductor Materials Design for Organic Complementary Circuits
  Usta, H.; Facchetti, A.; Marks, T. J. *Acc. Chem. Res.* **2011**, *44*, 501–510.
  Abstract:

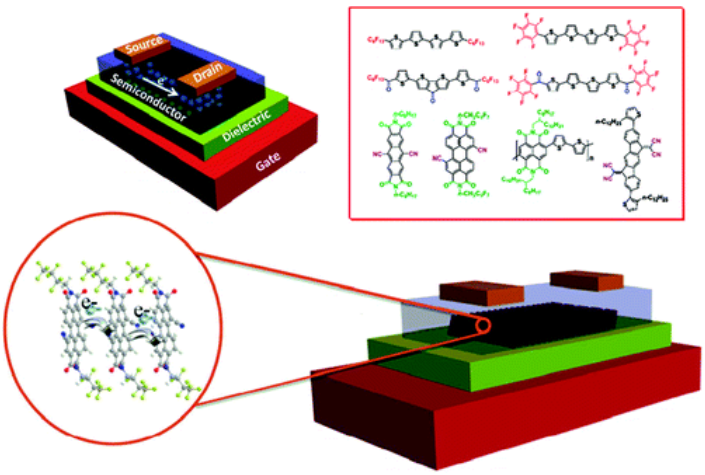

Organic semiconductors have unique properties compared to traditional inorganic materials such as amorphous or crystalline silicon. Some important advantages include their adaptability to low-temperature processing on flexible substrates, low cost, amenability to high-speed fabrication, and tunable electronic properties. These features are essential for a variety of next-generation electronic products, including low-power flexible displays, inexpensive radio frequency identification (RFID) tags, and printable sensors, among many other applications. Accordingly, the preparation of new materials based on π-conjugated organic molecules or polymers has been a central scientific and technological research focus over the past decade. Currently, *p*-channel (hole-transporting) materials are the leading class of organic semiconductors. In contrast, high-performance *n*-channel (electron-transporting) semiconductors are relatively rare, but they are of great significance for the development of plastic electronic devices such as organic field-effect transistors (OFETs).

In this Account, we highlight the advances our team has made toward realizing moderately and highly electron-deficient *n*-channel oligomers and polymers based on oligothiophene, arylenediimide, and (bis)indenofluorene skeletons. We have synthesized and characterized a "library" of structurally related semiconductors, and we have investigated detailed structure–property relationships through optical, electrochemical, thermal, microstructural (both single-crystal and thin-film), and electrical measurements. Our results reveal highly informative correlations between structural parameters at various length scales and charge transport properties.

We first discuss oligothiophenes functionalized with perfluoroalkyl and perfluoroarene substituents, which represent the initial examples of high-performance *n*-channel semiconductors developed in this project. The OFET characteristics of these compounds are presented with an emphasis on structure–property relationships. We then examine the synthesis and properties of carbonyl-functionalized oligomers, which constitute second-generation *n*-channel oligothiophenes, in both vacuum- and solution-processed FETs. These materials have high carrier mobilities and good air stability. In parallel, exceptionally electron-deficient cyano-functionalized arylenediimide derivatives are discussed as early examples of thermodynamically air-stable, high-performance *n*-channel semiconductors; they exhibit record electron mobilities of up to 0.64 $cm^2/V{\cdot}s$. Furthermore, we provide an overview of highly soluble ladder-type macromolecular semiconductors as OFET components, which combine ambient stability with solution processibility. A high electron mobility of 0.16 $cm^2/V{\cdot}s$ is obtained under ambient conditions for solution-processed films.

Finally, examples of polymeric *n*-channel semiconductors with electron mobilities as high as 0.85 $cm^2/V{\cdot}s$ are discussed; these constitute an important advance toward fully printed polymeric electronic circuitry. Density functional theory (DFT) computations reveal important trends in molecular physicochemical and semiconducting properties, which, when combined with experimental data, shed new light on molecular charge transport characteristics. Our data provide the basis for a fundamental understanding of charge transport in high-performance *n*-channel organic semiconductors. Moreover, our results provide a road map for developing functional, complementary organic circuitry, which requires combining *p*- and *n*-channel transistors.

- Zirconocene and Si-Tethered Diynes: A Happy Match Directed toward Organometallic Chemistry and Organic Synthesis
  Zhang, W.-X.; Zhang, S.; Xi, Z. *Acc. Chem. Res.* **2011**, *44*, 541–551.
  Abstract:

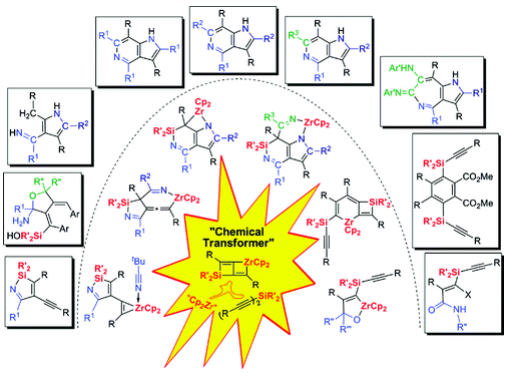

Characterizing reactive organometallic intermediates is critical for understanding the mechanistic aspects of metal-mediated organic reactions. Moreover, the isolation of reactive organometallic intermediates can often result in the ability to design new synthetic methods. In this Account, we outline synthetic methods that we developed for a variety of diverse Zr/Si organo-bimetallic

compounds and Si/N heteroatom–organic compounds through the detailed study of zirconacyclobutene–silacyclobutene fused compounds.

Two basic components are involved in this chemistry. The first is the Si-tethered diyne, which owes its rich reactive palette to the combination of the Si–C bond and the C≡C triple bond. The second is the low-valent zirconocene species $Cp_2Zr(II)$, which has proven very useful in organic synthesis. The reaction of these two components affords the zirconacyclobutene–silacyclobutene fused compound, which is the key reactive Zr/Si organo-bimetallic intermediate discussed here.

We discuss the three types of reactions that have been developed for the zirconacyclobutene–silacyclobutene fused intermediate. The reaction with nitriles (the C≡N triple bond) is introduced in the first section. In this one-pot reaction, up to four different components can be combined: the Si-tethered diyne can be reacted with three identical nitriles, with differing nitriles, or with a nitrile and other unsaturated organic substrates such as formamides, isocyanides, acid chlorides, aldehydes, carbodiimides, and azides. Several unexpected multiring, fused Zr/Si organo-bimetallic intermediates were isolated and characterized. A wide variety of *N*-heterocycles, such as 5-azaindole, pyrrole, and pyrroloazepine derivatives, were obtained. We then discuss the reaction with alkynes (the C≡C triple bond). A consecutive skeletal rearrangement, differing from that observed in the reactions with nitriles, takes place in this reaction. Finally, we discuss the reaction with the C═X substrates (where X is O or N), including ketones, aldehydes, and isocyanides. Oxa- and azazirconacycles are formed via a new skeletal rearrangement.

Our results show that the zirconocene and the Si-tethered diyne cooperate as a “chemical transformer” after treatment with various substrates, leading to a diverse range of cyclic Zr/Si organo-bimetallic compounds. This mechanism-derived synthesis of organometallic and organic compounds demonstrates that the investigation of metal-mediated reactions and the isolation of reactive organometallic intermediates not only contribute to the understanding of complex reactions but can also lead to the discovery of synthetically useful methods.

- Asymmetric Total Syntheses of (−)-Variabilin and (−)-Glycinol
  Calter, M. A.; Li, N. *Org. Lett.* **2011**, *13*, 3686–3689.
  Abstract:

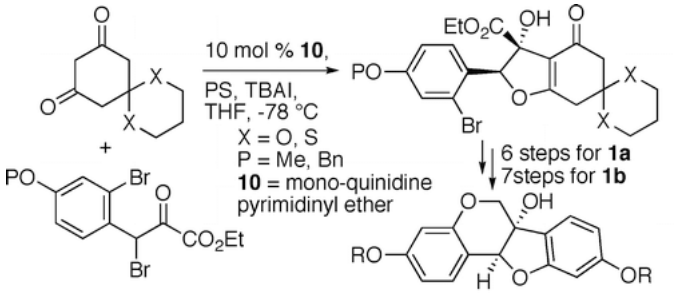

Total syntheses of (−)-variabilin and (−)-glycinol have been accomplished, using the catalytic, asymmetric “interrupted” Feist–Bnary reaction (IFB) as the key transformation to introduce both stereogenic centers. A monoquinidine pyrimidinyl ether catalyst affords the IFB products in over 90% ee in both cases. Other key steps include an intramolecular Buchwald–Hartwig coupling and a nickel-catalyzed aryl tosylate réduction

- A Formal Synthesis of SCH 351448
  Park, H.; Kim, H.; Hong, J. *Org. Lett.* **2011**, *13*, 3742–3745.

Abstract:

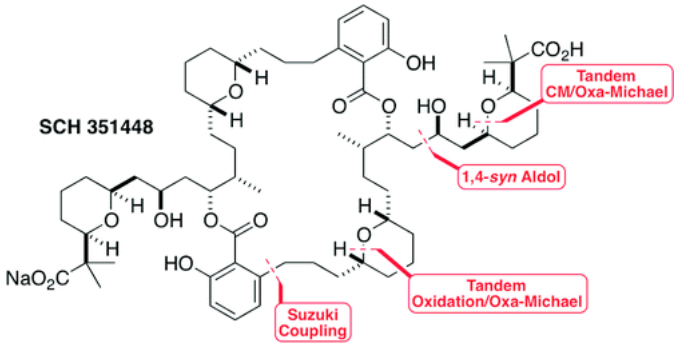

An efficient formal synthesis of SCH 351448 was accomplished through the tandem cross-metathesis (CM)/oxa-Michael, the 1,4-*syn* aldol, the tandem oxidation/oxa-Michael, and the Suzuki coupling reaction.

- Chemical functionalisation of silicon and germanium nanowires
  Collins, G.; Holmes, J. D. *J. Mater. Chem.* **2011**, *21*, 11052-11069.
  Abstract:

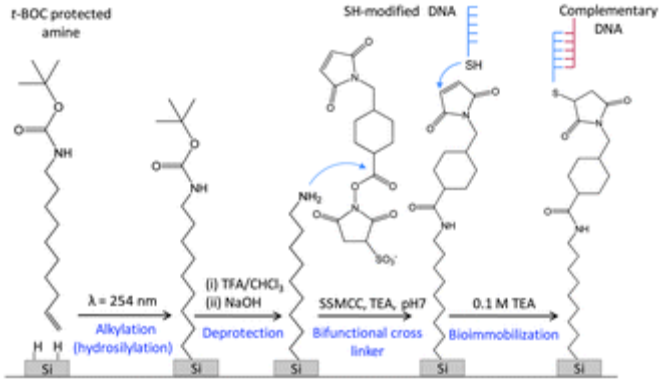

The reduced dimensionality of nanowires implies that surface effects significantly influence their properties, which has important implications for the fabrication of nanodevices such as field effect transistors and sensors. This review will explore the strategies available for wet chemical functionalisation of silicon (Si) and germanium (Ge) nanowires. The stability and electrical properties of surface modified Si and Ge nanowires is explored. While this review will focus primarily on nanowire surfaces, much has been learned from work on planar substrates and differences between 2D and nanowire surfaces will be high-lighted. The possibility of band gap engineering and controlling electronic characteristics through surface modification provides new opportunities for future nanowire based applications. Nano-sensing is emerging as a major application of modified Si nanowires and the progress of these devices to date is discussed.

- *In situ* preparation of fluorescent polyaniline nanotubes doped with perylene tetracarboxylic acids
  Rana, U.; Chakrabarti, K.; Malik, S. *J. Mater. Chem.* **2011**, *21*, 11098-11100.
  Abstract:

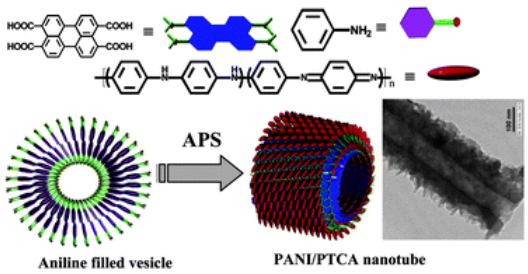

Herein, we report an easy preparation of polyaniline (PANI) nanotubes in the presence of perylene tetracarboxylic acid acting as a dopant. These tubes are crystalline and fluorescent in nature as a result of controlled confinement of dopant molecules in the tubes.